ChemComm

Accepted Manuscript

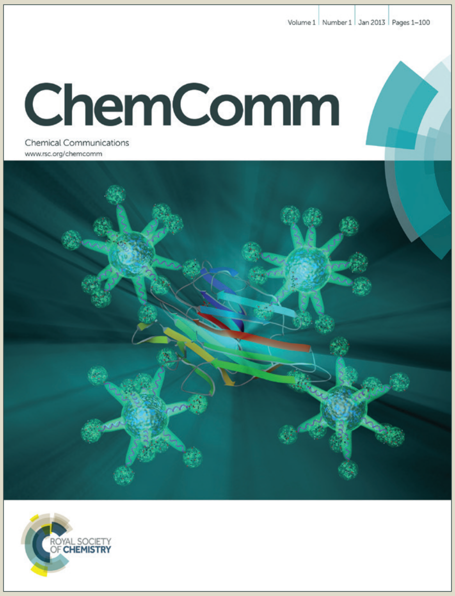

ROYAL SOCIETY OF CHEMISTRY

www.rsc.org/chemcomm

ChemComm RSCPublishing

COMMUNICATION

A low bandgap asymmetrical squaraine for high-performance solution-processed small molecule organic solar cells †

Cite this: DOI: 10.1039/x0xx00000x

Received 00th January 2014,
Accepted 00th January 2014

DOI: 10.1039/x0xx00000x

www.rsc.org/chemcomm

Daobin Yang, ‡[a] Qianqian Yang, ‡[b] Lin Yang, [a] Qian Luo, [a] Yao Chen, [a] Youqin Zhu, [b] Yan Huang, *[a] Zhiyun Lu *[a] and Suling Zhao *[b]

A novel asymmetrical squaraine ASQ-5 bearing indoline as end capper exhibits low bandgap of 1.43 eV and broad absorption band in the Vis-NIR region of 550-850 nm in thin film, hence renders solution-processed organic solar cells with an impressive J_{sc} of up to 11.03 mA cm^{-2} and an excellent PCE of 4.29%.

In recent years, small molecular organic solar cells (SMOSC) have attracted great interest because of their advantages over their polymer counterparts, including well-defined molecular structure, facile material synthesis, definite molecular weight and high purity without batch to batch variations,[1] while bulk-heterojunction (BHJ) device structure is demonstrated to be more effective to achieve high power conversion efficiency (PCE).[2] Among the multifarious kinds of small molecular photovoltaic materials that have been developed, squaraine dyes have demonstrated strong potential for use in OSC,[3] since they possess high molar extinction coefficients, intense absorption in Vis-NIR spectral regions, excellent photochemical and photophysical stability,[4] so far, the record PCE for solution-processed squaraine-based BHJ-OSC is as high as 5.50%.[5] It is noted that the squaraine dye used in this device has a symmetrical molecular structure (SQ, D-A-D), however, asymmetrical squaraines (ASQ, D-A-D') are more promising candidates relative to SQ because of their much better molecule structural tenability.[6]

Nevertheless, the PCE of ASQ-based BHJ-SMOSC is relatively low (0.20-2.05%), which should be mainly ascribed to their low V_{oc} (0.24-0.69 V) and J_{sc} (1.40-9.05 mA cm^{-2}).[7] Very recently, we have reported a ASQ photovoltaic material ASQC bearing 9-carbazyl as end capper, obtaining the highest V_{oc} (1.12 V) of single BHJ SMOSC based on small molecule donors because of its extremely deep HOMO level of -5.46 eV.[8] However, this ASQ material (ASQC) exhibited a medium bandgap (1.65 eV), which is attributed to the weak electron-donating capability of 9-carbazyl and large dihedral angle (48°) between the dihydroxyphenyl ring and 9-carbazyl core, this is one of the most important reason for limiting increasing of J_{sc} (7.00 mA cm^{-2}), resulting in the PCE of corresponding BHJ photovoltaic devices is also relatively low (2.82 %). Therefore, we attempt to develop ASQ with a low bandgap by introducing a suitable end capper. Indoline, a constructional units widely used in dye-sensitized solar cells materials,[10] but never used in OSC materials as a end capper, is incorporated into the 4-amino-2,6-dihydroxy phenyl group owing to its much stronger electron-donating capability and smaller steric hindrance than 9-carbazyl,[11] so that the resulted compound ASQ-5 might possess a low bandgap, resulting in an excellent J_{sc} and PCE. Additionally, another compound ASQ-6 with 1,2,3,4-tetrahydroquinoline instead of indoline is constructed, 1,2,3,4-tetrahydroquinoline exhibits the similar electron-donating capability as indoline, while they show the different steric conformation.[12] Thus, the effect of different end cappers, indoline *vs.* 1,2,3,4-tetrahydroquinoline, on the optoelectronic properties of ASQ has been investigated too.

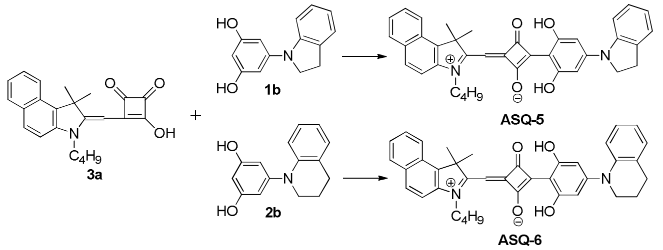

Scheme 1 Synthetic routes to the target molecules.

The synthetic routes to the target molecules are illustrated in Scheme 1. All the synthetic and characterization details could be found in electronic supplementary information (ESI†). The benzo[*e*]indole semi-squarylium compound 3a condensed with aromatic compound 1b or 2b to obtain the asymmetrical squaraine ASQ-5 or ASQ-6 with high yield nearly 80%, which possess an excellent solubility in common organic solvents, such as chloroform and 1,2-dichlorobenzene (> 40 mg mL^{-1}). Additionally, high quality films of the two compounds could be achieved through spin-coating, suggesting that they are very suitable for solution-processing.

The molecular structures of the two compounds (*vide* Fig. 1, Table S1, ESI†) are determined by X-ray diffraction on single crystals. In the two compounds, the squarate cores and phenyl moieties both

Table 2 Optical and electrochemical properties of the ASQ

Compound	Absorption λ_{max} (nm)		FWHM (nm)		E_g^{opt}	E^{onset}_{ox}	HOMO	LUMO
	Solution (log ε)	Film	Solution	Film	eV	V	eV	eV
ASQ-5	678 (5.37)	725, 657	39	166	1.43	0.29	-5.09	-3.66
ASQ-6	671 (5.36)	713, 648	39	146	1.49	0.29	-5.09	-3.60

show similar quasi-coplanar conformations (*vide* Table 1, $\varphi_1 < 4°$) due to the existence of strong hydrogen bonding interactions (O···H-O). The π-system of ASQ-5 is nearly planar conformation as there is only a small twist (φ_2=3.8°) between the dihydroxyphenyl ring and indoline core, leading to more extended conjugation systems of ASQ-5,[13] while ASQ-6 displays a remarkably twisted conformation with φ_2 of 56.5°. The much larger φ_2 in ASQ-6 is mainly attributed to its steric hindrance originating from H_1 and H_2. According to the packing diagrams of ASQ-5 (shown in Fig. S1, ESI†), the distance between two neighboring molecules is much shorter than that of ASQ-6 (3.38 Å *vs.* 3.84 Å), the shorter π-π distance results from the much smaller twist (φ_2) of ASQ-5, indicating of the presence of significant π-π interaction, which may facilitate the charge carrier transportation.[14]

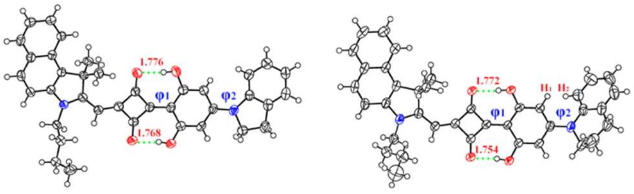

Fig. 1 ORTEP diagrams for ASQ-5 (left) and ASQ-6 (right).

Table 1 Conjugated backbone conformation and packing of the ASQ determined from single crystal structures (φ: dihedral angle)

Compound	φ_1 (°)	φ_2 (°)	Distance (Å)
ASQ-5	1.3	3.8	3.38
ASQ-6	3.9	56.5	3.84

The UV-vis absorption spectra of the two compounds in solution and thin film are shown in Fig. 2, and data are summarized in Table 2. In solution, the maximum absorption peak of ASQ-6 was 671 nm, which was slightly blue-shifted 7 nm compared with that of ASQ-5 (678 nm), which is due to the existence of a remarkably twisted conformation (φ_2=56.5°). Additionally, both of them exhibit a considerably high molar extinction coefficient (log ε > 5.00). In comparison with their absorption spectra in solution, the ICT absorption bands of ASQ-5 and ASQ-6 in films were significantly red-shifted, extending to 725 and 713 nm, respectively. It is noteworthy that absorption bands of the two compounds in solution display the identical full width half maxima (FWHM) of 39 nm, while the thin film absorption band of ASQ-5 is broader than that of ASQ-6 (FWHM, 166 nm *vs.* 146 nm), which should be attributed to its more coplanar conformation than that of ASQ-6, this broadening is important for OSC since it leads to improved spectral overlap with the solar irradiance spectrum. Determined by UV-vis absorption onset of the films, the optical bandgap of ASQ-5 is lower than ASQ-6 (1.43 eV *vs.* 1.49 eV), which is the lowest bandgap based on photovoltaic materials of asymmetrical squaraines dyes.[15]

According to cyclic voltammetry measurment (Table 2 and Fig. S2, ESI†), both of the two compounds exhibit a similar reversible one-electron oxidation wave at 0.29 V, the HOMO energy levels of two compounds are calculated to be -5.09 eV, which are mainly attributed to their similar electron-donating capability of indoline and 1,2,3,4-tetra-hydroquinoline. The LUMO energy levels of ASQ-5 and ASQ-6 are calculated to be -3.66 and -3.60 eV, respectively, which are deduced from the HOMO levels and corresponding optical bandgaps.[16]

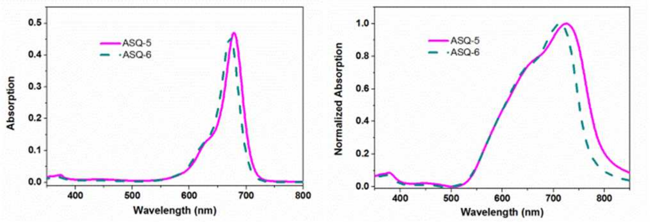

Fig. 2 Absorption spectra of ASQ in solution (left) and thin film (right).

According to the experimental and calculation results, the hole mobility of the as-prepared ASQ-5 and ASQ-6 neat films are 2.00×10^{-5} cm^2 V^{-1} s^{-1} and 1.80×10^{-5} cm^2 V^{-1} s^{-1} (Fig. S3, ESI†), respectively, while the hole mobility of the donor-acceptor blending films are reduced to 1.71×10^{-6} cm^2 V^{-1} s^{-1} and 1.36×10^{-6} cm^2 V^{-1} s^{-1} (Fig. S4, ESI†), respectively. The difference in hole mobility observed for ASQ-5 and ASQ-6 can most likely be ascribed to differences in molecule packing. ASQ-5 has a shorter intermolecular distance than that of ASQ-6 (3.38 Å *vs.* 3.84 Å), which should result in slightly higher carrier mobility.

To evaluate the photovoltaic performance of the two compounds, devices with structure of glass/ ITO/ MoO_3 (80 Å)/ ASQ: $PC_{71}BM$ (800 Å)/ LiF (8 Å)/ Al (1000 Å) have been fabricated. OSC devices were optimized with respect to donor-acceptor blend ratios and thermo-annealing, the representative photovoltaic data of the devices are summarized in Table S2, S3 (ESI†), and current density-voltage (*J-V*) curves are shown in Fig. S5, S6 (ESI†). The optimized blend ratio of ASQ: $PC_{71}BM$ are 1:5, the photoactive layer annealing temperature is 70 ºC for 20 min, and the corresponding *J-V* curves and key data of the devices are given in Fig. 3 and Table 3.

Table 3 Photovoltaic performances of the ASQ

Active layer (w/w)	V_{oc} (V)	J_{sc} (mA cm^{-2})	FF	PCE (%)
ASQ-5: $PC_{71}BM$=1: 5	0.82	10.29	0.45	3.80
ASQ-5: $PC_{71}BM$=1: 5 [a]	0.81	11.03	0.48	4.29
ASQ-6: $PC_{71}BM$=1: 5	0.83	8.97	0.46	3.42
ASQ-6: $PC_{71}BM$=1: 5 [a]	0.82	9.50	0.47	3.66

a. annealing at 70 °C for 20 min.

In comparison with the ASQ-6-based device, ASQ-5-based OSC device shows much higher J_{sc} (10.29 mA cm^{-2} *vs.* 8.97 mA cm^{-2}) without thermo-annealing. As J_{sc} is not only determined by the absorption of donor material, but also closely related to hole mobility and the morphology between donor-acceptor blend films.[17] Thus, the morphological properties of these photoactive blend films have been investigated by AFM (Fig. S7, ESI†), both ASQ-5 and ASQ-6-based blend films show similar morphologies and quite smooth surfaces with root-mean-square (RMS) of 0.24 nm and 0.22 nm, respectively. Therefore, the higher J_{sc} should be assigned to the broader absorption band and higher hole mobility of ASQ-5 relative to ASQ-6, and the results are consistent with their EQE curves (shown in Fig. 3), the EQE value of ASQ-5-based device is higher than that of ASQ-6 in the region of 350-710 nm, and broader in the region of 710-800 nm. Additionally, both of them display satisfactory V_{oc} (~ 0.82 V) and high FF (~ 0.47) based on the SMOSC devices of ASQ,[7] thus the PCE of ASQ-5 and ASQ-6-based SMOSC devices are as high as 3.80% and 3.42% without any post-treatment, respectively.

Upon thermal annealing, the device performance of the two ASQ are enhanced, the PCE increase to 4.29% for ASQ-5 and 3.66% for ASQ-6. The much higher PCE is a result of much improved J_{sc} (11.03 mA cm^{-2} *vs.* 9.50 mA cm^{-2}), this results are consistent with EQE values (shown in Fig. 3). To the best of our knowledge, ASQ-5-based BHJ-SMOSC devices exhibit the highest record J_{sc} (11.03 mA cm^{-2}) for any asymmetrical squaraines dyes.[7] Further optimization of morphology on the active layer are underway to gain more information and will be reported elsewhere.

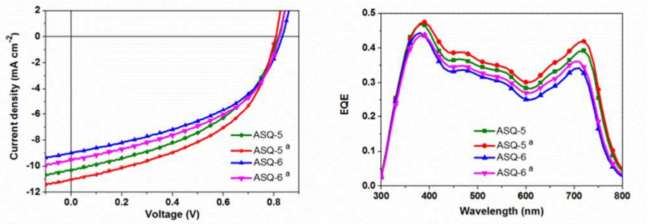

Fig. 3. *J-V* curve of photovoltaic devices (left) and EQE curves (right).

In conclusion, a novel asymmetrical squaraine ASQ-5 bearing indoline as end capper with compromised low bandgap of 1.43 eV with broad absorption band and HOMO energy level of -5.09 eV has been synthesized. Compared with ASQ-6 bearing 1,2,3,4-tetrahydroquinoline as end capper, ASQ-5 exhibits a lower bandgap, broader absorption band, much shorter intermolecular distance, and higher carrier mobility, which is attributed to its more planar conformation. Therefore, solution-processed ASQ-5-based BHJ-SMOSC shows an impressive J_{sc} of 11.03 mA cm^{-2} and an excellent PCE of 4.29%, while that based on ASQ-6 exhibits J_{sc} of 9.50 mA cm^{-2} and PCE of 3.66%. These preliminary works demonstrate that ASQ-5 is a perspective electron donor candidate, and indoline-modification strategy may pave a new way for achieving photovoltaic devices with greatly improved J_{sc} and PCE.

We acknowledge the financial support for this work by the National Natural Science Foundation of China (project No. 21190031 and 21372168) and New Century Excellent Talents in University (grant No. NCET-10-0220). We are grateful to the Analytical & Testing Center of Sichuan University for providing single crystal X-ray diffraction data for the objective molecules.

Notes and references

[a] *Key Laboratory of Green Chemistry and Technology (Ministry of Education), College of Chemistry, Sichuan University, Chengdu 610064, P. R. China. E-mail: huangyan@scu.edu.cn (Y. Huang); luzhiyun@scu. edu.cn (Z. Lu);*

[b] *Key Laboratory of Luminescence and Optical Information (Ministry of Education), Institute of Optoelectronics Technology, Beijing Jiaotong University, Beijing 100044, P. R. China. E-mail: slzhao@bjtu.edu.cn (S. Zhao)*

† Electronic supplementary information (ESI) available: synthetic procedure, crystal data and packing, CV curves, charge carrier mobility calculation method, photovoltaic device data and AFM image. CCDC 986049 and 986050.

‡ The first two authors contributed equally to this work.

1 (a) Y. Lin, Y. Li and X. Zhan, *Chem. Soc. Rev.*, 2012, **41**, 4245; (b) A. Mishra and P. Bäuerle, *Angew. Chem. Int. Ed.*, 2012, **51**, 2020.
2 (a) J. Zhou, X. Wan, Y. Liu, Y. Zuo, Z. Li, G. He, G. Long, W. Ni, C. Li, X. Su and Y. Chen, *J. Am. Chem. Soc.*, 2012, **134**, 16345; (b) A. K. K. Kyaw, D. H. Wang, D. Wynands, J. Zhang, T.-Q. Nguyen, G. C. Bazan and A. J. Heeger, *Nano. Lett.*, 2013, **13**, 3796.
3 (a) G. Wei, X. Xiao, S. Wang, K. Sun, K. J. Bergemann, M. E. Tompson and S. R. Forrest, *Acs Nano*, 2012, **6**, 972; (b) S. L. Lam, X. Liu, F Zhao, C-L. K. Lee and W. L. Kwan, *Chem. Commun.*, 2013, **49**, 4543; (c) J.-S. Huang, T.Goh, X. Li, M. Y. sfeir, E. A. Bielinski, S. Tomasulo, M. L. Lee, N. Hazari and A. D. Taylor, *Nat. Photon.*, 2013, **7**, 479; (d) G. Chen, H. Sasabe, Y. Sasaki, H. Katagiri, X.-F. Wang, T. Sano, Z. Hong, Y. Yang and J. Kido, *Chem. Mater.*, 2014, **26**, 1356.
4 L. Beverina and P. Salice, *Eur. J. Org. Chem.*, 2010, **2010**, 1207.
5 G. Wei, S. Wang, K. Sun, M. E. Thompson and S. R. Forrest, *Adv. Energy Mater.*, 2011, **1**, 184.
6 (a) S. S. Pandey, R. Watanabe, N. Fujikawa, Y. Ogomi, Y. Yamaguchi and S. Hayase, *Proc. Of SPIE*, 2011, **8111**, 811116; (b) J. Fabian, *Chem. Rev.*, 1992, **92**, 1197.
7 (a) U. Mayerhöffer, K. Deing, K. Gruβ, H. Braunschweig, K. Meerholz and F. Würthner, *Angew. Chem. Int. Ed.*, 2009, **48**, 8776; (b) L. Beverina, R. Ruffo, M. M. Salamone, E. Ronchi, M. Binda, D. Natali and M. Sampietro, *J. Mater. Chem.*, 2012, **22**, 6704; (c) S. So, H. Choi, H. M. Ko, C. Kim, S. Paek, N. Cho, K. Song, J. K. Lee and J. Ko, *Sol. Energy Mater. Sol. Cells*, 2012, **98**, 224; (d) K. C. Deing, U. Mayerhöffer, F. Würthner and K. Meerholz, *Phys. Chem. Chem. Phys.,* 2012, **14**, 8328.
8 D. Yang, Q. Yang, L. Yang, Q. Luo, Y. Huang, Z. Lu and S. Zhao, *Chem. Commun.,* 2013, **49**, 10465.
9 S. Wang, L. Hall, V. V. Diev, R. Haiges, G. Wei, X. Xiao, P. I. Djurovich, S. R. Forrest and M. E. Thompson, *Chem. Mater.*, 2011, **23**, 4789.
10 (a) T. Horiuchi, H. Miura, K. Sumioka and S. Uchida, *J. Am. Chem. Soc.,* 2004, **126**, 12218; (b) S. Ito, H. Miura, S. Uchida, M. Takata, K. Sumioka, P. Liska, P. Comte, P. Péchy and M. Grätzel, *Chem. Commun.*, 2008, 5194; (c) X. Liu, Z. Cao, H. Huang, X. Liu, Y. Tan, H. Chen, Y. Pei and S. Tan, *J. Power Sources*, 2014, **248**, 400.
11 (a) S. Chen, L. Vasquez, B. C. Noll and M. R. DuBois, *Organometallics*, 1997, **16**, 1757; (b) Y. Wu, X. Zhang, W. Li, Z. Wang, H. Tian and W. Zhu, *Adv. Energy Mater.*, 2012, **2**, 149; (c) K. Funabiki, H. Mase, Y. Saito, A. Otsuka, A. Hibino, N. Tanaka, H. Miura, Y. Himori, T. Yoshida, Y. Kubota and M. Matsui, *Org. Lett.*, 2012, **14**, 1246; (d) Y. Wu and W. Zhu, *Chem. Soc. Rev.*, 2013, **42**, 2039.
12 A. S. K. Hashmi, M. Rudolph, J. W. Bats, W. Frey, F. Rominger and T. Oeser, *Chem. Eur. J.*, 2008, **14**, 6672.
13 J. Hou, M. H. Park, S. Zhang, Y. Yao, L. M. Chen, J. H. Li and Y. Yang, *Macromolecules*, 2008, **41**, 6012.
14 J. Liu, B. Walker, A. Tamayo, Y. Zhang and T.-Q. Nguyen, *Adv. Funt. Mater.*, 2013, **23**, 47.
15 (a) 3b; (b) 7b; (c)7c; (d) 8.
16 J. Dai, K. Zhou, M. Li, H. Sun, Y. Chen, S. Su, X. Pu, Y. Huang and Z. Lu, *Dalton Trans.*, 2013, **42**, 10559.
17 (a) A. J. Heeger, *Adv. Mater.*, 2014, **26**, 10; (b) V. D. Mihailetchi, H. X. Xie, B. de Boer, L. J. A. Koster and P. W. M. Blom, *Adv. Funt. Mater.*, 2006, **16**, 699; (c) H. Hoppe, M. Niggemann, C. Winder, J. Kraut, R. Hiesgen, A. Hinsch, D. Meissner and N. S. Sariciftci, *Adv. Funt. Mater.*, 2004, **14**, 1005.